Supporting Information

Photophysics of a Ruthenium Complex with a π-Extended Dipyridophenazine Ligand for DNA Quadruplex Labeling

Julian Schindler,[a,b] Philipp Traber,[a] Linda Zedler,[b] Ying Zhang,[a,b] Jean-François Lefebvre,[c,d] Stephan Kupfer,[a] Stefanie Gräfe,[a] Martine Demeunynck,[c] Murielle Chavarot-Kerlidou,[d] and Benjamin Dietzek*,[a,b]

[a] Institute of Physical Chemistry and Abbe Center of Photonics, Friedrich Schiller University Jena, Helmholtzweg 4, 07743 Jena, Germany. Phone: +49 3641 206332; Fax: +49 3641 206399; E-mail: benjamin.dietzek@leibniz-ipht.de

[b] Department Functional Interfaces, Leibniz Institute of Photonic Technology Jena (IPHT), Albert-Einstein-Straße 9, 07745 Jena, Germany.

[c] Univ. Grenoble Alpes, CNRS, DPM, 38000 Grenoble, France.

[d] Laboratoire de Chimie et Biologie des Métaux, Univ. Grenoble Alpes, CNRS, CEA, 38000 Grenoble, France.

1. Resonance Raman Spectroscopy

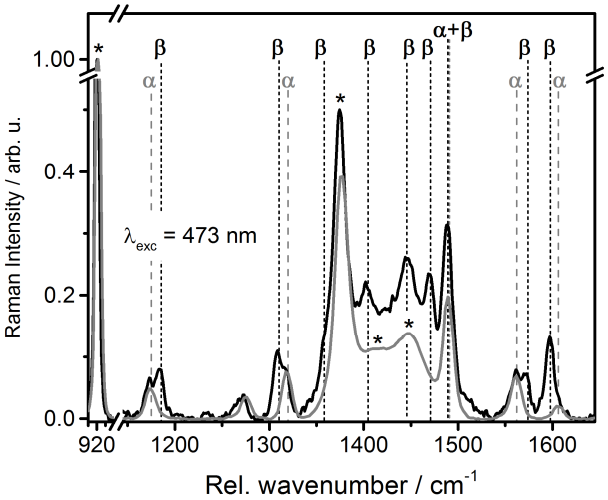

Figure S1: Assignment of the RR bands which are characteristic for vibrations of the of the bpy ligands (α) and the dppz moiety (β). These peaks are assigned by comparing the RR spectra of **2** (black line) and $[Ru(bpy)_3](PF_6)_2$ (grey line) (in ACN, excitation at 473 nm) and by taking the reported RR spectrum of $[Ru(dppz)_3]^{2+}$ into account.[1]

2. Electrochemistry

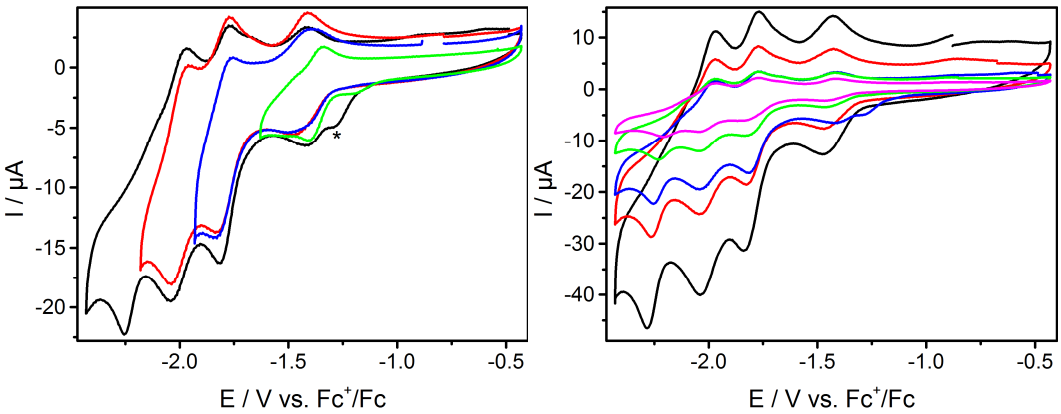

Figure S2: Cyclic voltammograms (CVs) of **1** (0.5 mM) on a glassy carbon electrode in a 0.1 M $TBAPF_6$ solution in DMF. Left Figure: CVs recorded at 100 mV/s (the process labelled with * corresponds to the reduction of traces of oxygen). Right Figure: CVs recorded at different scan rates (25 (magenta line), 50 (green line), 100 (blue line), 200 (red line) and 500 mV/s (black line)).

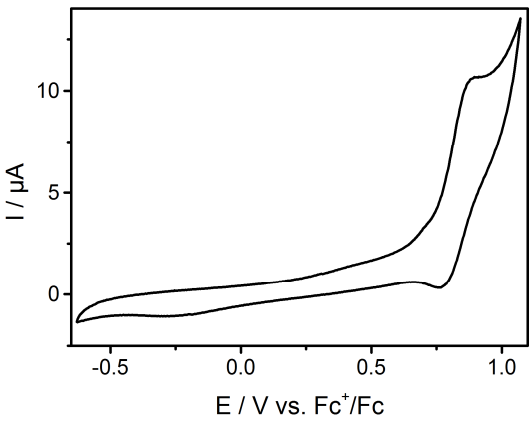

Figure S3: Cyclic voltammogram of **1** (1.0 mM) recorded at 100 $mV.s^{-1}$ on a platinum electrode in a 0.1 M $TBAPF_6$ solution in DMF.

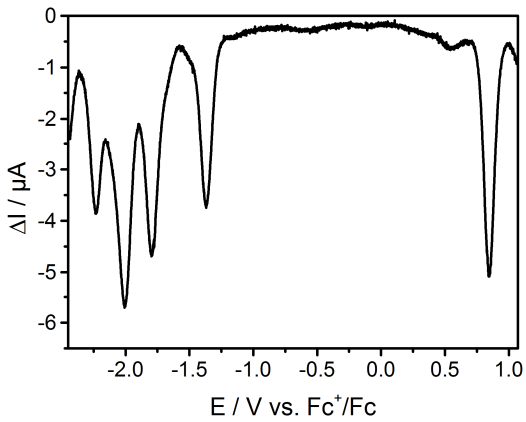

Figure S4: Differential pulse voltammogram (cathodic scan) of **1** (1.0 mM) recorded on a glassy carbon electrode in a 0.1 M $TBAPF_6$ solution in DMF. (DPV parameters: P_{Height} = 10 mV, P_{Width} = 25 ms, S_{Height} = -1 mV, S_T = 100 ms)

3. UV/Vis-Spectroelectrochemistry

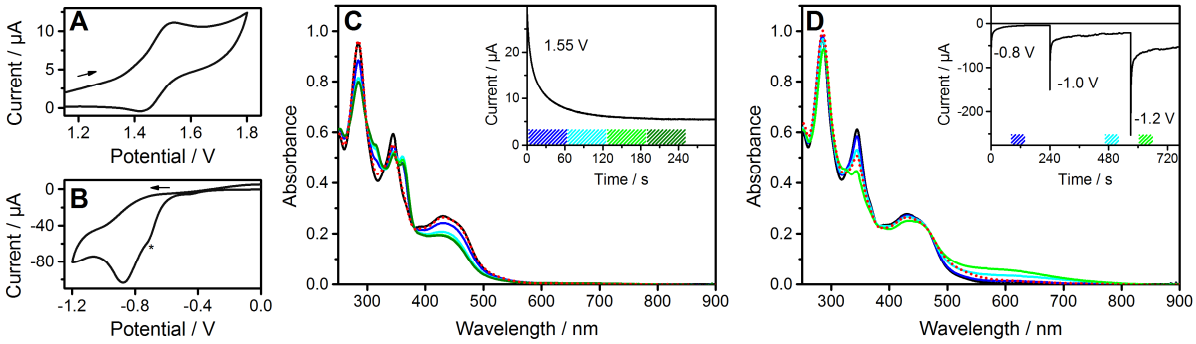

Figure S5: Cyclic voltammograms measured in the SEC cuvette showing the first one-electron oxidation (A) and first one-electron reduction process for **1** (B, the shoulder labelled with * corresponds to the reduction of traces of oxygen). The absorption spectrum of the parent oxidation state (black line), i.e. the non-reduced / non-oxidized **1**, respectively, are shown together with the absorption spectra observed during the formation of the singly oxidized (C) and singly reduced species (D). Formation of these species is achieved by applying a constant potential. The respective chronoamperograms are shown in the inset. The applied potentials as well as the time necessary to collect each absorption spectrum is highlighted in each graph using the same color code. To check for reversibility of the oxidation and reduction process, an absorption spectrum was measured after re-reduction / re-oxidation at 0 V vs. Ag/AgCl pseudo-reference (red dotted line), respectively. UV/Vis-SEC investigations in 0.1 M tetrabutylammonium tetrafluoroborate/acetonitrile. All potentials are measured against a Ag/AgCl pseudo-reference electrode.

4. Nanosecond time-resolved transient absorption and emission spectroscopy

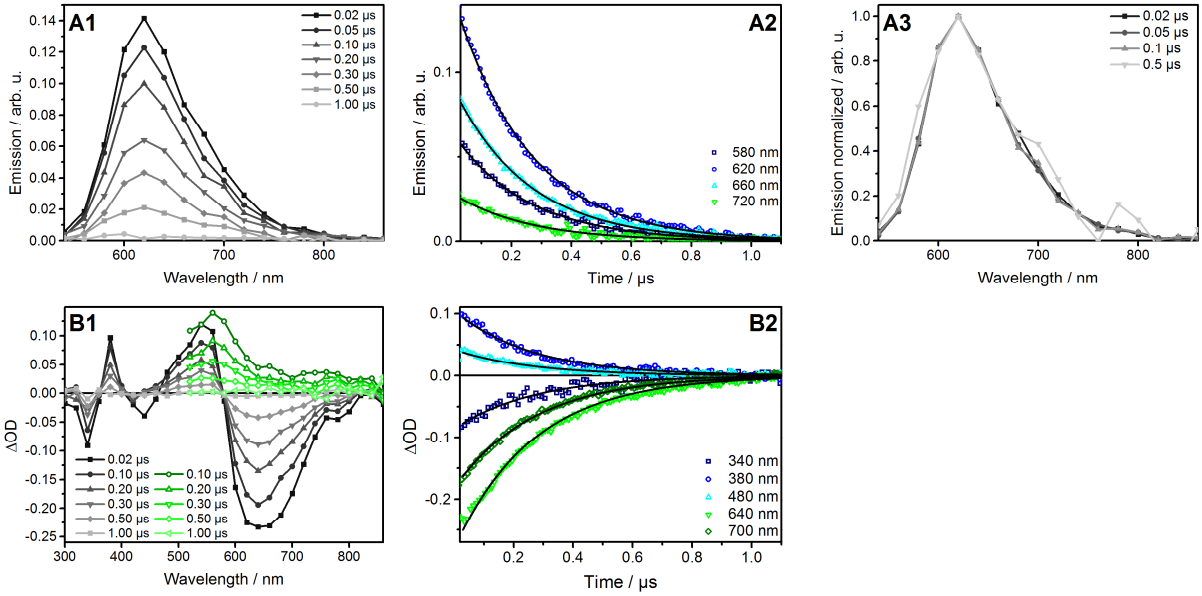

Figure S6: The ns-Em (A1 and A2) and ns-TA spectra of **1** (B1, filled grey symbols) in air-equilibrated ACN upon 450-nm excitation. The ns-TA spectra are corrected for spontaneous emission, which contributes between 550 to 800 nm (B1, green non-filled symbols). Selected kinetic traces (symbols) and mono-exponential fitting curves (solid lines) – obtained by a global fitting routine – are presented for the emission (A2, τ = 0.25 µs) and transient-absorption data (B2, τ = 0.26 µs). Transient emission spectra are normalized to the maximum intensity (A3).

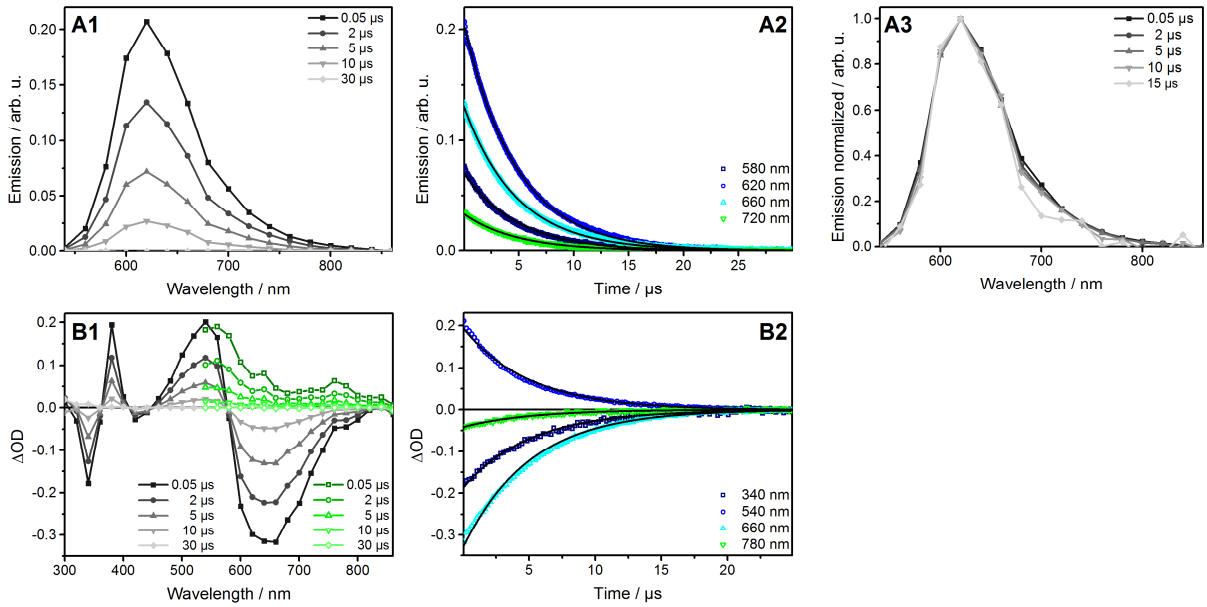

Figure S7: The ns-Em (A1 and A2) and ns-TA spectra of **1** (B1, filled grey symbols) in oxygen-free ACN upon 450-nm excitation. The ns-TA spectra are corrected for spontaneous emission which contributes between 550 to 800 nm (B1, green non-filled symbols). Selected kinetic traces (symbols) and mono-exponential fitting curves (solid lines) – obtained by a global fitting routine – are presented for the emission (A2, τ = 4.8 µs) and transient-absorption data (B2, τ = 5.0 µs). Transient emission spectra are normalized to the maximum intensity (A3).

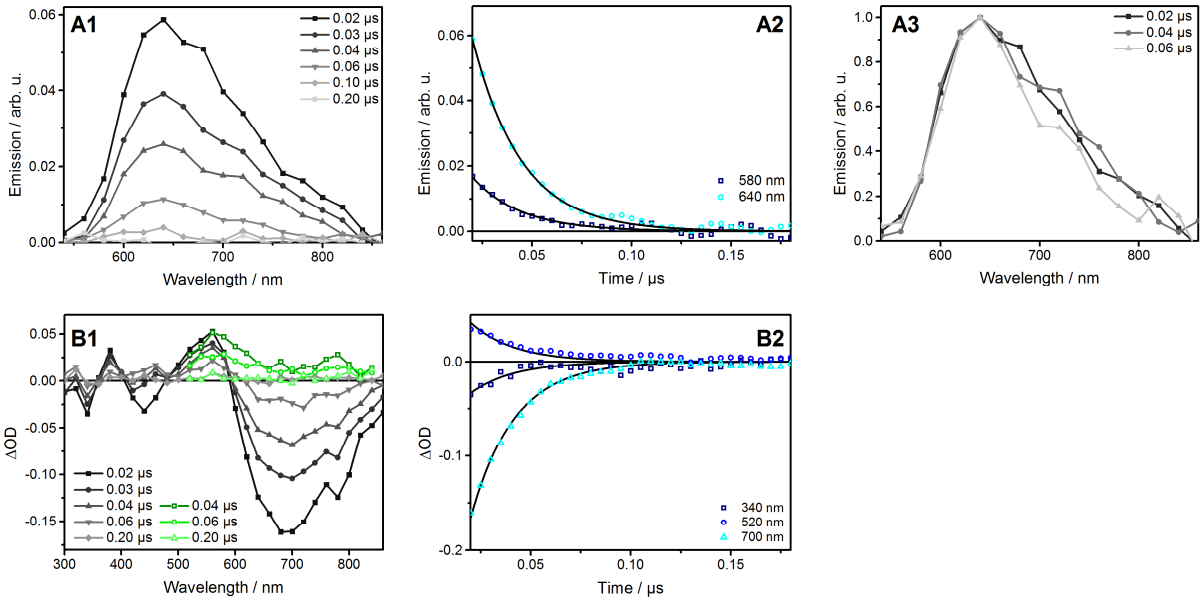

Figure S8: The ns-Em (A1 and A2) and ns-TA spectra of **1** (B1, filled grey symbols) in an air-equilibrated 1:1 mixture of ACN/water upon excitation at 450 nm. The ns-TA spectra are corrected for spontaneous emission (B1, green non-filled symbols). Selected kinetic traces (symbols) and mono-exponential fitting curves (solid lines) – obtained by a global fitting routine – are presented for the emission (A2, τ = 24 ns) and transient-absorption data (B2, τ = 22 ns). Transient emission spectra are normalized to the maximum intensity (A3).

5. Femtosecond time-resolved transient absorption spectroscopy

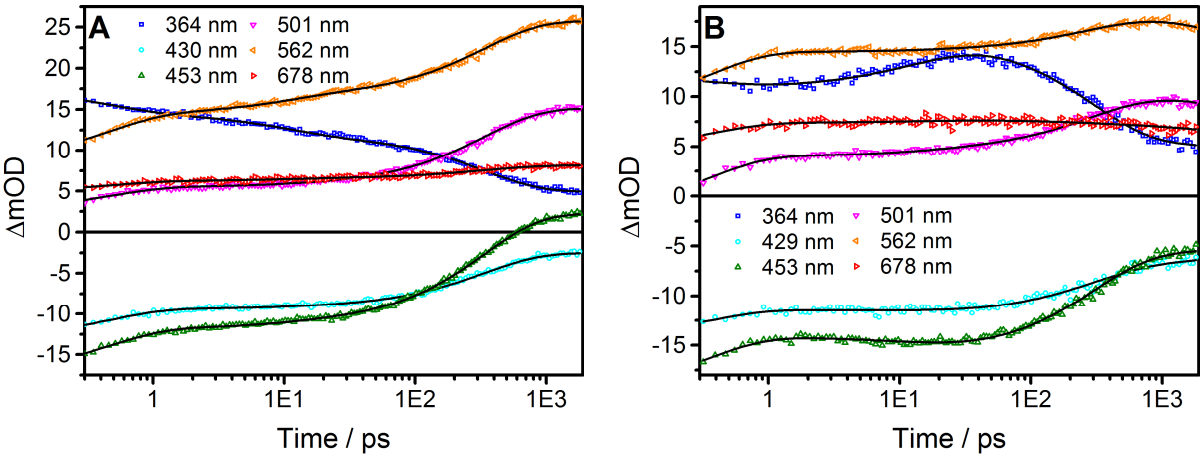

Figure S9: Kinetic traces for **1** in ACN (A) and in a 1:1 mixture of ACN/water (B) at selected wavelengths (symbols) upon 400-nm excitation. The fitting curves obtained from the global fit are shown with solid lines.

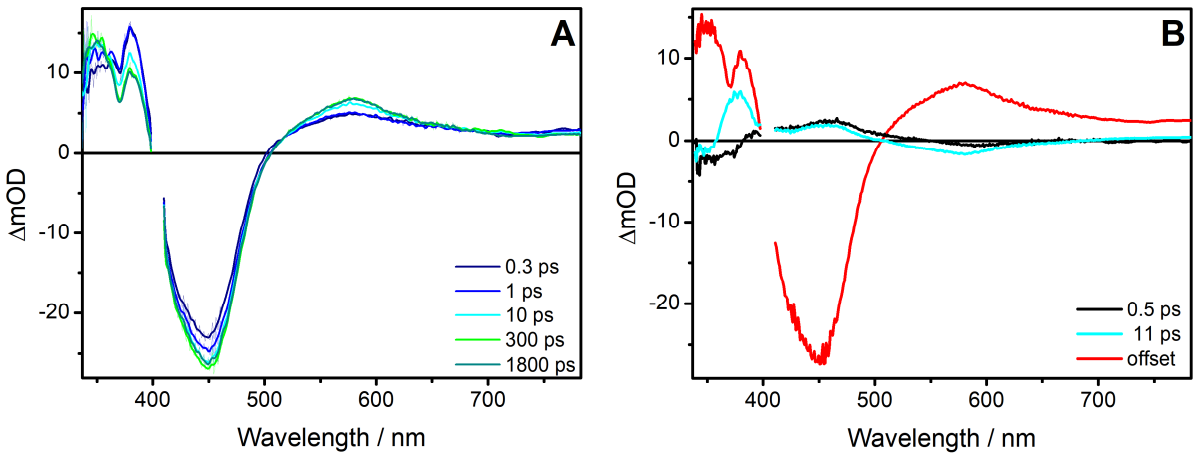

Figure S10: fs-TA spectra for **2** in ACN recorded upon pumping at 403 nm (A). Decay-associated spectra and values of the corresponding time constants (B) obtained from global analysis of the transient spectra. The constant offset (red line, B) does not decay on the timescales accessible with the fs-TA setup and corresponds to the long-lived state. Scattering of the pump beam has been omitted for clarity.

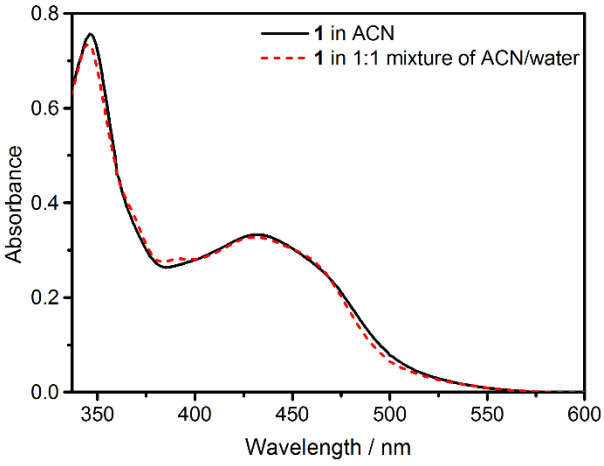

Figure S11: Ground-state absorption spectra of **1** in ACN (black solid line) and in a 1:1 mixture of ACN/water (red dashed line).

6. TDDFT calculations: singlet state of 1

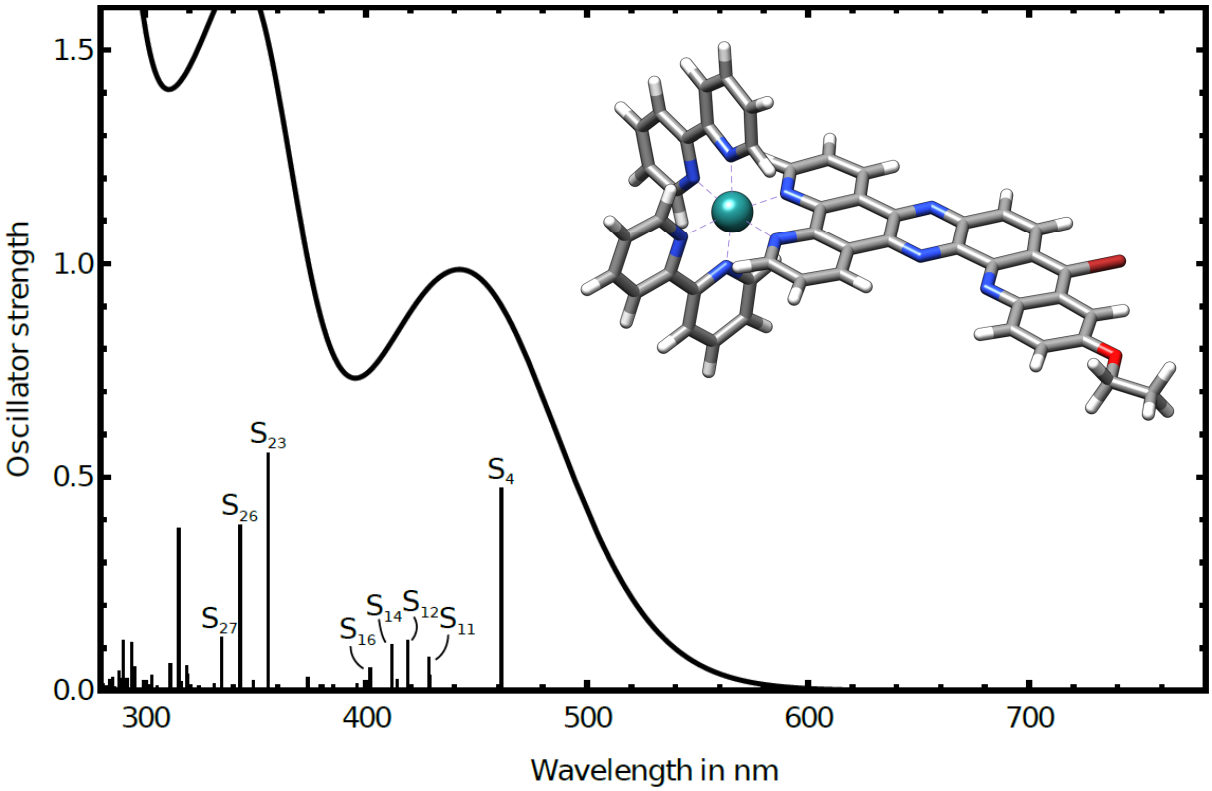

Figure S12: Simulated UV/Vis absorption spectrum of **1** in ACN. The calculated oscillator strengths of the singlet excited states are represented by black bars. Gaussian functions with a full width at half maximum of 0.28 eV are employed to broaden the transitions. The optimized singlet ground state structure is presented in the inset. See Table S1 for electronic transitions.

Table S1: Electronic transitions for the singlet ground state of **1**: Calculated vertical singlet-singlet excitation energies (E), wavelengths (λ), wavenumbers ($\tilde{\nu}$) oscillator strengths (f) and eigenvalues of $\langle s^2 \rangle$ of the main excited states in the UV and visible range. Transitions are visualized by the accompanying shift of charge density from blue to red (CDD).

Excitations						Hole	CDD	Electron
	λ / nm	E / eV	$\tilde{\nu}$ / cm^{-1}	f	$\langle s^2 \rangle$		From blue to red	
S_4	461	2.69	21682	0.4709	0.000	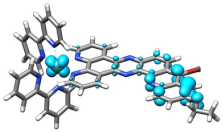	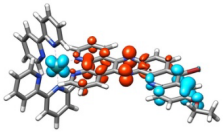	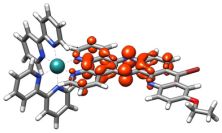
S_{11}	428	2.89	23348	0.0743	0.000	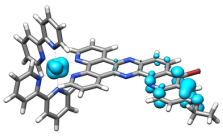	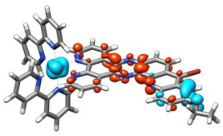	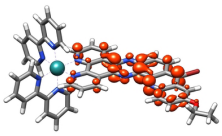
S_{12}	419	2.96	23882	0.1140	0.000	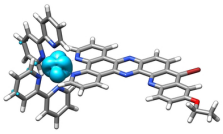	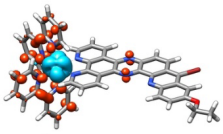	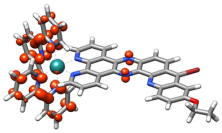
S_{14}	412	3.01	24280	0.1052	0.000	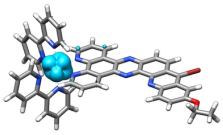	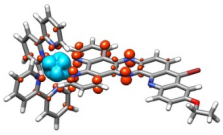	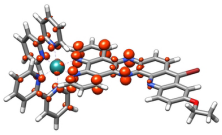
S_{16}	402	3.09	24884	0.0497	0.000	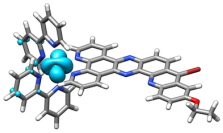	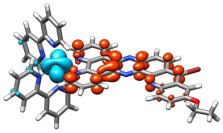	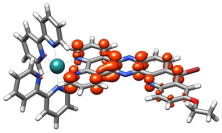
S_{23}	356	3.48	28102	0.5546	0.000	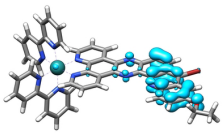	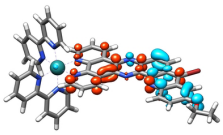	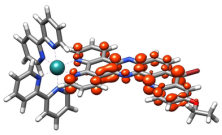
S_{26}	343	3.62	29157	0.3843	0.000	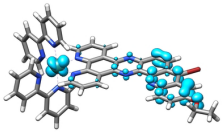	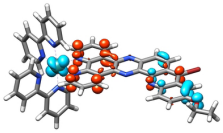	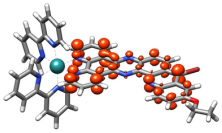
S_{27}	335	3.70	29870	0.1221	0.000	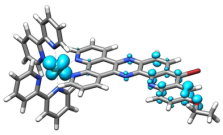	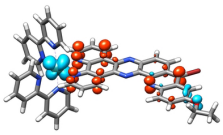	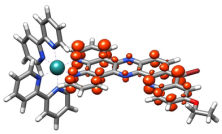

7. TDDFT calculations: triplet state of 1

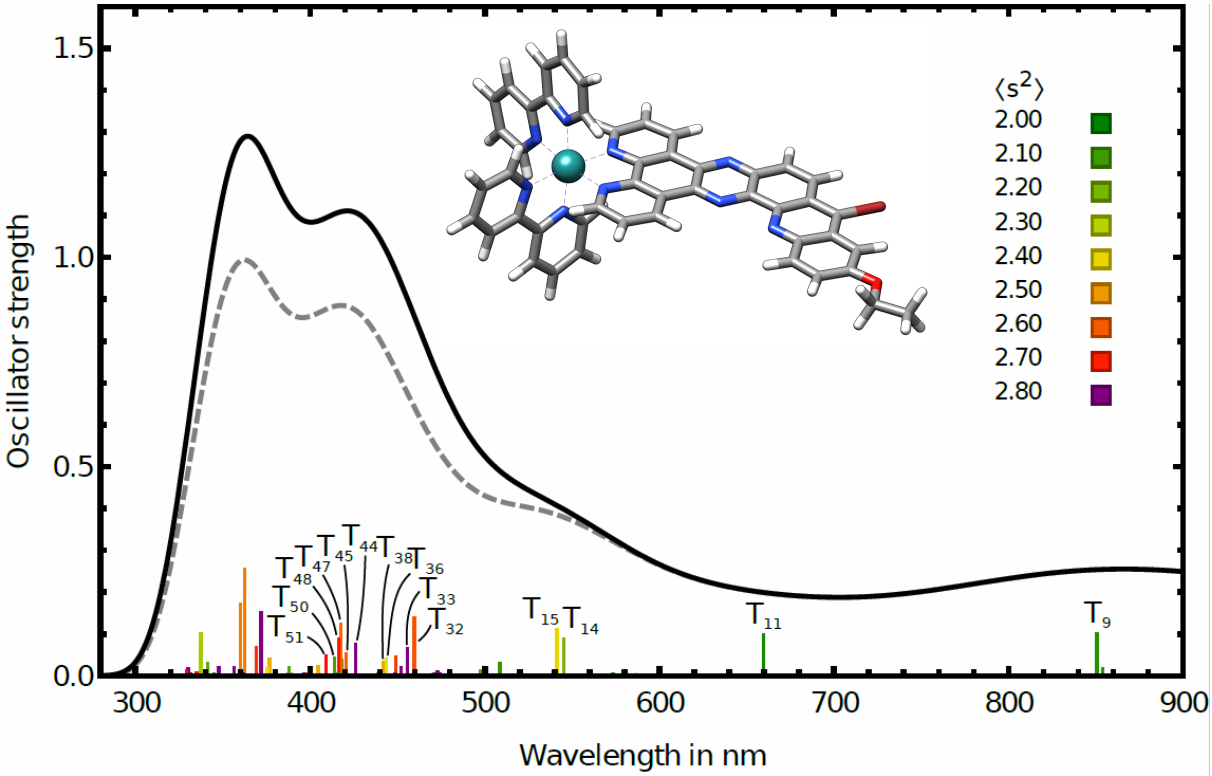

Figure S13: Simulated UV/Vis absorption spectrum of **1** in ACN starting from the optimized geometry of the lowest triplet state. The calculated oscillator strengths of the spin-allowed triplet-triplet excited states are represented by black bars. Gaussian functions with a full width at half maximum of 0.28 eV are employed to broaden the transitions: including all excited triplet states (black solid line) and including only states with a spin-contamination lower than $\langle s^2 \rangle = 2.75$ (grey dashed line). The optimized triplet ground state structure is presented in the inset. See Table S2 for electronic transitions.

Table S2: Electronic transitions for the triplet ground state of **1**: Calculated vertical triplet-triplet excitation energies (E), wavelengths (λ), wavenumbers ($\tilde{\nu}$) oscillator strengths (f) and eigenvalues of $\langle s^2 \rangle$ of the main excited states in the UV and visible range. Transitions are visualized by the accompanying shift of charge density from blue to red (CDD).

Excitations						Hole	CDD	Electron
	λ / nm	E / eV	$\tilde{\nu}$ / cm^{-1}	f	$\langle s^2 \rangle$		From blue to red	
T_9	851	1.46	11755	0.1011	2.062	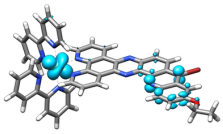	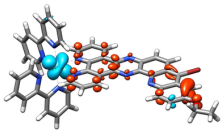	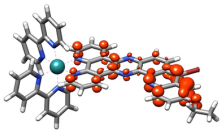
T_{11}	660	1.88	15162	0.0988	2.037	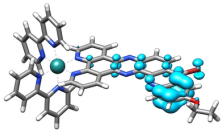	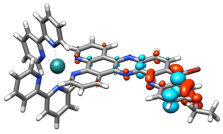	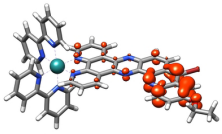
T_{14}	545	2.27	18346	0.0885	2.194	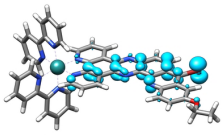	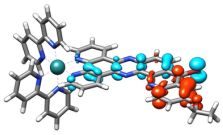	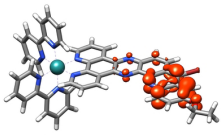
T_{15}	541	2.29	18471	0.1108	2.399	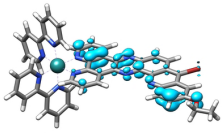	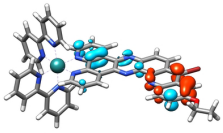	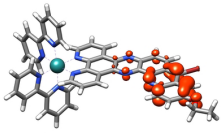
T_{32}	460	2.70	21759	0.1377	2.620	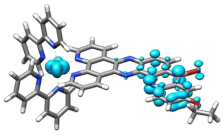	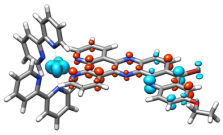	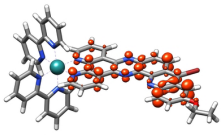
T_{33}	456	2.72	21950	0.0644	3.490	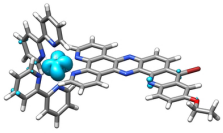	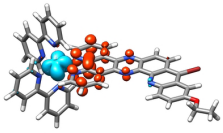	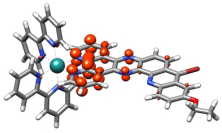
T_{36}	449	2.76	22278	0.0461	2.662	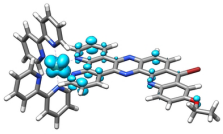	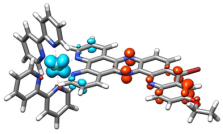	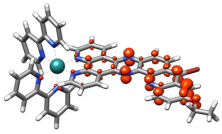
T_{38}	444	2.80	22543	0.0403	2.373	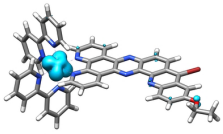	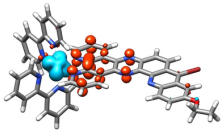	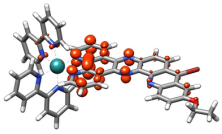
T_{44}	426	2.91	23463	0.0748	2.856	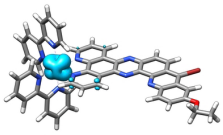	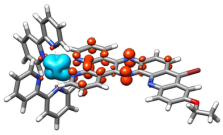	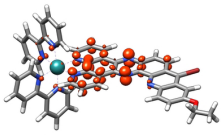
T_{45}	420	2.95	23785	0.0532	2.605	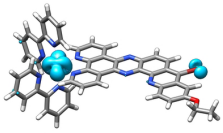	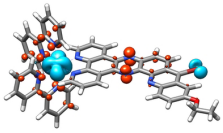	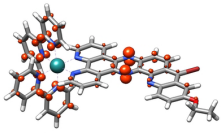
T_{47}	417	2.97	23956	0.1228	2.586	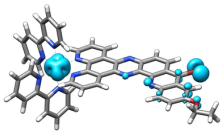	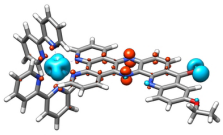	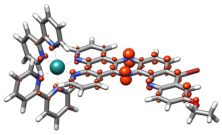
T_{48}	416	2.98	24021	0.0888	2.715	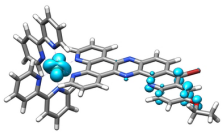	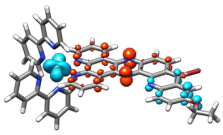	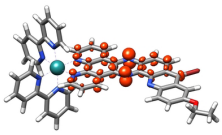

Excitations						Hole	CDD	Electron
	λ / nm	E / eV	$\tilde{\nu}$ / cm^{-1}	f	$\langle s^2 \rangle$	From blue to red		
T_{50}	414	3.00	24164	0.0412	2.122	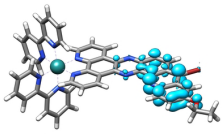	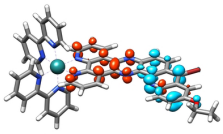	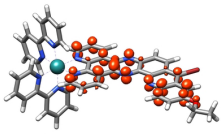
T_{51}	409	3.03	24437	0.0470	2.741	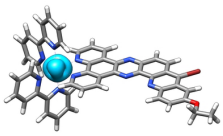	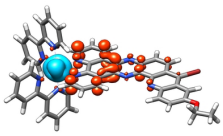	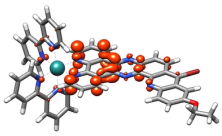

References

(1) Coates, C. G.; Jacquet, L.; McGarvey, J. J.; Bell, S. E.; Al-Obaidi, A. H.; Kelly, J. M. Resonance Raman probing of the interaction between dipyridophenazine complexes of Ru(II) and DNA. *J. Am. Chem. Soc.* **1997**, *119*, 7130–7136.